RADIATION PERFORMANCE ENHANCEMENT OF A MICROSTRIP ANTENNA BASED ON EBG AT WIMAX BANDS

Yahiea Alnaiemy[1] and Lajos Nagy[2]

This article presents 3×3 *Electromagnetic Band Gap (EBG) array mounted on top of a truncated slotted square patch antenna for gain and radiation and aperture efficiency enhancements. The proposed EBG unit cell is inspired from the Split Ring Resonator (SRR) geometry. The proposed EBG array is located at approximately of* $0.7\lambda_\circ$*, where* $\lambda_\circ$ *is the free space wavelength at 5.2 GHz, from the antenna patch. Equivalently, a circuit model is derived to compute the S-parameters of the EBG array and compared against those obtained from the numerical simulations. Later, the performance of the EBG based antenna is investigated numerically and experimentally in terms of* $|S_{11}|$ *spectra, gain, aperture efficiency, and radiation patterns. The EBG array and antenna dimensions are investigated to maximize the boresight gain at 5.2 GHz for WiMAX applications. On a FR-4 substrate with maximum dimensions of* $70 \times 70 \times 1.6$ mm^3*, the optimal antenna design is fabricated. A significant gain enhancement is achieved, from 3.4 dBi to 8.95 dBi at 5.2 GHz, after introduced the EBG array. The proposed antenna bandwidth covers the frequencies from 5.15 GHz to 5.83 GHz with an excellent improvement in the aperture efficiency about 31%. A significant Half Power Beamwidth (HPBW) reduction at E-plan and H-plane from 107.27° to 86.6° and from 124.37° to 66.8°, respectively, is achieved.*

Keywords: EBG, boresight gain, aperture efficiency, HPBW

1. Introduction

Last decades, metamaterials registered remarkable interests due to their unique electromagnetic properties [1]. Metamaterials are artificial structures can be engineered periodically to control permittivity (ϵ) and permeability (μ) over certain bands [2]. For this, many researchers invented novel applications based on SRR and EBG structures [3]. For example, the concept of perfect lenses for antenna gain enhancement was developed first by John [4].

[1] Ph.D Student, Budapest University of Technology and Economics Budapest, Hungary, e-mail: yahiea@hvt.bme.hu

[1] Lecturer, College of Science, University of Diyala, Diyala, Iraq

[2]Professor, Budapest University of Technology and Economics Budapest, Hungary

Later, the use of high impedance metasurfaces for mutual coupling reduction between antennas was developed for multiple input multiple output (MIMO) technologies for wireless communication [5]. However, the use of SRRs still very limited to specific applications due to its highly resonance structures [6] specifically when integrated with printed circuit boards [7]. In the same aspect, several researchers attempted to utilize metamaterials to improve antenna bandwidth, gain, aperture efficiency, and radiation properties over a limited size [8]-[21]. For instance, the authors in [8] extended the microstrip antenna bandwidth to ultra-wideband (UWB) by using metamaterial double side planar periodic structures. The authors in [9] were demonstrated a Uniplanar Compact-Photonic Band Gap (UC-PBG) structure with conventional square microstrip patch antenna to improve the antenna gain and size reduction. Two planar arrays with 9×9 UC-PBG unit cells were placed on the microstrip antenna radiating patch with a gap of 130 mm to obtained gain 7.8 dBi at 2.6 GHz. In [10], a microstrip antenna based on a complementary SRR (CSRR) loaded on the ground plane was investigated for gain enhancement. An endfire antenna with enhanced gain over a wideband was designed with SRR structure in [11]. A Hexagonal SRR based on compact UWB was developed in [12] for pH sensing between the frequency bands from 7.43 GHz up to 11.79 GHz. Four layers of SRR arrays were arranged to investigate the gain enhancement [13]. The authors in [14] enhanced the gain for UWB antenna by utilizing two layers of square SRRs placed on the antenna patch and the ground plane for microwave imaging systems. The authors in [15] explored four layers of nested SRRs mounted on top of a microstrip patch antenna for gain enhancement. An enhanced gain microstrip antenna based EBG structure was developed in [16]. The authors in [17] proposed an EBG based patch antenna of improved boresight gain from 5.6 dBi to 11.1 dBi for Wi-Fi applications using multiple corrugated and non-corrugated SRRs. A triangular SRR with wire strip were implemented to enhance the microstrip antenna gain [18]. The authors in [19] integrated six plates with four SRR arrays based on a microstrip antenna to improve the antenna gain by 2 dB and the bandwidth by 5% at the S-band. In reference [20], the researchers obtained the circular polarization of a rectangular patch microstrip with a single feed. A single layer of negative metamaterial was implemented as radiating patch to achieve a compacted size antenna for different applications [21].

In this paper, a uniform planar array of 3×3 EBG layer placed on top of a microstrip antenna is investigated to improve the antenna performance in terms of $|S_{11}|$ spectra, bandwidth, radiation patterns, boresight gain, and aperture efficiency. The combination of the proposed EBG array with the microstrip antenna could suit different wireless applications over the frequency range from 5.12 GHz to 5.83 GHz including the WiMAX networks. The proposed microstrip antenna based on EBG array structure is simulated, fabricated,

tested, and measured. The simulation is carried out using Computer Simulation Technology Microwave Studio (CSTMW) based on Finite Integration Technique (FIT) formulations. The paper is organized as follows: In Section 2, we present the design methodology and numerical setup for the EBG unit cell, truncated slotted patch antenna, and microstrip antenna design based on EBG array structure. A systematic approach to obtain the optimal antenna design is presented in Section 3. Sections 4 and 5 discuss the microstrip antenna performance with and without the EBG layer numerically and experimentally, respectively. Finally, the paper is concluded in Section 6.

2. **Design methodology**

In this section, a systematic design methodology that is suggested to reach the proposed antenna design is discussed. The proposed EBG is designed as two concentrated rings with two different radii. The patch geometry is designed as a truncated slotted square. The distance between the EBG array and the patch structure is optimized parametrically to reach the maximum realized gain and aperture efficiency. The design methodology can be divided into three main parts: First, the EBG unit cell design with best periodicity and separation distance to achieve a -μ_r at the desired frequency band is discussed. Next, the proposed antenna based on a truncated slotted square patch is designed to operate at 5.2 GHz. The effects of applying the EBG structure to the antenna performance at 5.2 GHz is discussed in the last part.

2.1. **EBG Design**

EBG is defined as a sub-wavelength metamaterial with negative -ϵ_r and μ_r at the frequency band of interest [2]. The resonance frequency of the EBG structure is usually affected by several parameters including the EBG unit cell dimensions and the separation between the unit cells in their structure lattice [22]. Therefore, Time Domain Solver (TDS) of CSTMW based on FIT [23] formulations is invoked to investigate the proposed EBG behavior in term of S-parameters. The proposed EBG structure, see Fig.1 is placed inside a fictitious waveguide to extract the S-parameters. Two waveguide ports are applied to obtain a quasi-TEM like modes [24] by considering the upper and lower walls of the waveguide as Perfect Electrical Conductors (PECs) and the side walls as Perfect Magnetic Conductors (PMCs). All the geometrical details are listed in Table 1.

Table 1

The Geometrical dimensions of the EBG unit cell

Parameter	Dimension (mm)	Parameter	Dimension (mm)
w1	3	r2	5.5
w2	3	g1	1.2
r1	8	g2	2

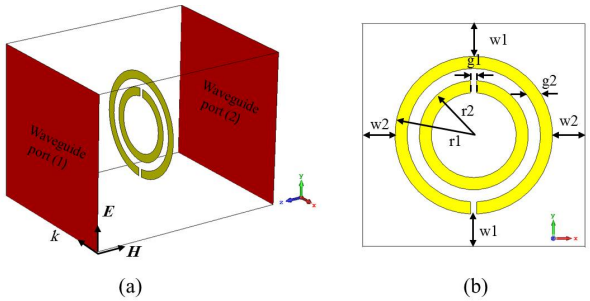

Fig. 1. EBG unit cell:(a) CSTMWS numerical setup and (b) unit cell dimension details

It is good to mention that the proposed unit cell structure is shaped as SRR geometry. However, the authors treated this unit cell as an EBG structure when mounted it inside the waveguide parallel to the waveguide port plane. Therefore, the expected results would be different done the traditional electromagnetic properties of SRR. Based on that the resultant medium would light enough with low impedance to allow the electromagnetic transmission with a certain refection; this can be explained from the following equation 1 [1].

$$\eta = \eta_o \sqrt{\frac{\mu_r}{\epsilon_r}} \tag{1}$$

Now the proposed EBG unit cell property is evaluated in terms of the dispersion diagram. The proposed EBG structure dispersion diagram for the Transverse Electric (TE) and Transverse Magnetic (TM) modes at the first Brillion zone is indicated in Fig. 2 (a). The simulated results obtained indicate a specific band gap at the frequency of interested. In the frequency range of interest the structure is seen as supporting a fundamental TM mode that is mainly longitudinal to the direction of propagation mainly transversal to propagation path followed by TE mode [1]. The propagation in TM mode below 2.4 GHz, while in TE mode below 5.4 GHz, it may be deemed prohibited.

In the simulation, a tetrahedral mesh with an adaptive mesh scheme is involved based on Time Domain Solver (TDS) of CSTMW. The EBG structure is discussed as an LC circuit. The equivalent capacitances are indicated to the EBG gap distance and the split gap distance where they are in series connected [5]. The inductor is equivalent to the magnetic field that is stored inside the rings [5]. The load resistance is given by the free space impedance (377Ω) as indicated in Fig. 2 (b). The values of the proposed equivalent circuit are listed in Table 2.

The authors would like to bring the attention that the evaluated lumped element parameters in Table 2 are obtained from a tuning study in Advanced

Table 2

EBG Effective Circuit Parameters

Parameter	Value	Parameter	Value	Parameter	Value
L_{ring}	1.3 nH	C	2.87pF	C_{gap}	19.3 pF

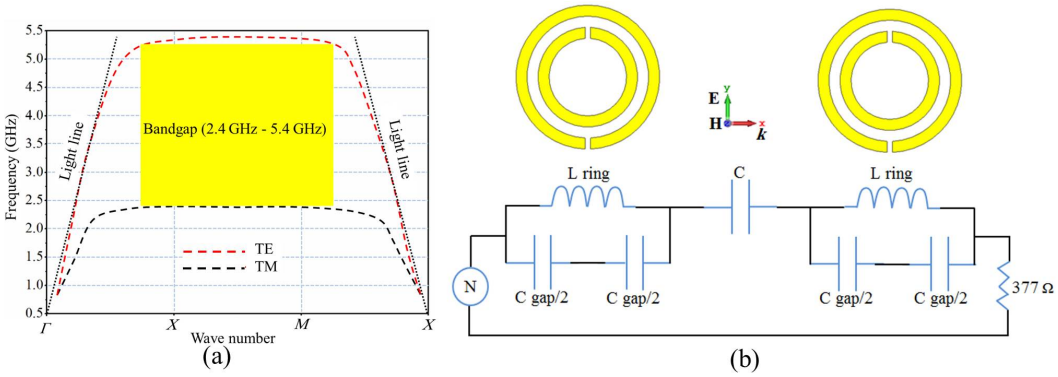

Fig. 2. (a) Dispersion diagram of the proposed EBG with band gap, and (b) Equivalent circuit of the EBG structure

Design System (ADS) software package. The EBG resonant frequency can be obtained directly from the equivalent circuit, see Fig. 2(b), as expressed in equation 2 [1]. Therefore, the variation in the resonant frequency could happen when the gap width and the rings radii vary. Therefore, to obtain the operating frequency at 5.2 GHz, a parametric study is conducted to realize the values of the capacitor and the inductor (C_{gap} and L_{ring}).

$$f_o = \frac{1}{2\pi\sqrt{L_{\text{ring}}C_{\text{gap}}}} \tag{2}$$

A parametric study based on gap width (g1) of the slotted EBG ring for the suggested EBG is conducted to determine the operating resonance frequency, which leads to the desired negative permittivity (-ϵ_r) and negative refractive index (-n) in the interested frequency band. Figure 3(a) shows the parametric study by changing g1 from 0.1 mm to 0.7 mm with a step of 0.1 mm. It is observed that $|S_{21}|$ spectra are significantly affected by g1 value variation. Therefore, the resonant frequency is shifted from 4.85 GHz at g1= 0.1 mm to 5.28 GHz at g1= 0.7 mm. It is observed from the obtained results at g1= 0.5 mm, the matching impedance is significantly enhanced.

Figure 3(b) illustrates the real part of μ_r , ϵ_r, and n parameters which are obtained to demonstrate that the proposed EBG has -μ_r only at 5.2 GHz.

Referring to Fig. reffig3(b), the displayed $|S_{21}|$ spectrum indicates -μ_r with ϵ_r at 5.2 GHz. The EBG array is printed on a flexible FR4 substrate of 0.55 mm thickness. Figure 3(c) shows the S-parameters of the proposed

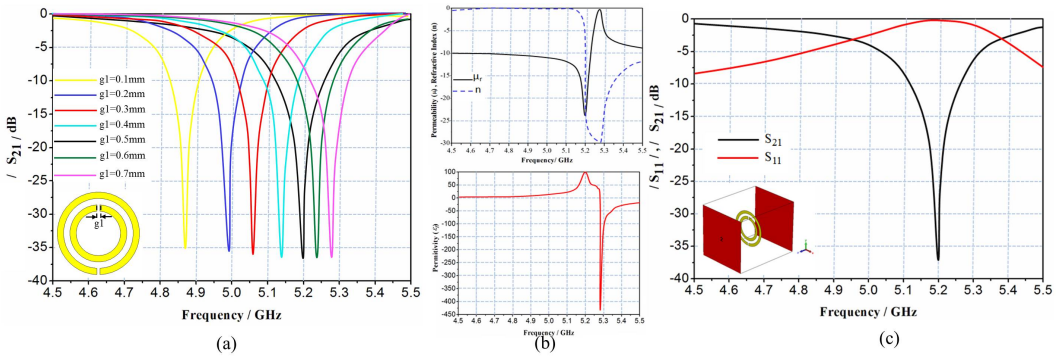

Fig. 3. (a) Variation of resonance frequency of the EBG unit cell for changing the parameter of g1, (b)Effective medium parameter of EBG unit cell μ_r, n, ϵ_r, and (c)Obtained S-parameters spectra.

EBG structure. From the extracted S-parameters for the proposed EBG, the maximum achieved $|S_{21}|$ is found at 5.2 GHz.

2.2. Patch Design

The proposed patch antenna geometry is designed at 5.2 GHz. The patch antenna structure is mounted on an FR-4 substrate with a maximum dimensions of 70×70 $(\text{mm})^2$ and a thickness of 1.6 mm as presented in Fig.4. The radiating patch element is excited directly by a coaxial cable. More geometrical details are listed in Table 3.

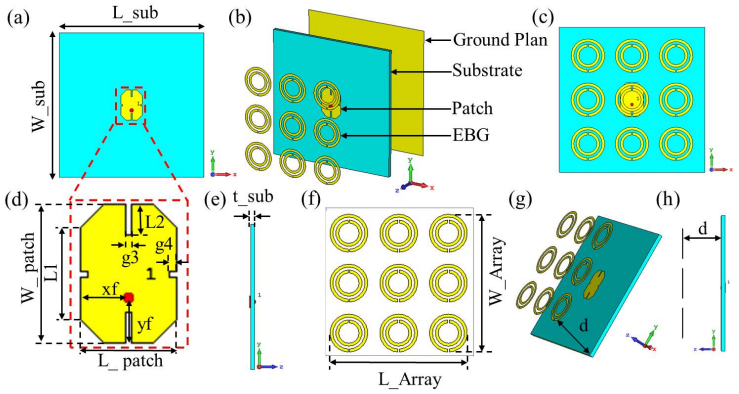

Fig. 4. Geometrical details of the proposed antenna and EBG array structure.

The systematic study is conducted based on CSTMWS simulations. The design procedure is started with a conventional rectangular patch antenna backed with a solid ground plane. Next, the corners of the microstrip patch

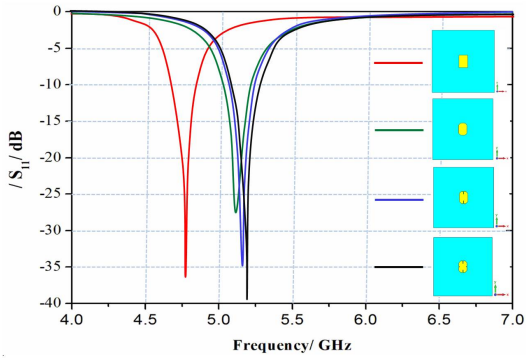

Fig. 5. $|S_{11}|$ spectra of the proposed patch geometries.

are truncated in order to improve $|S_{11}|$ spectra. Then, the rectangular slots are etched from the upper and lower sides of the proposed patch antenna. Finally, the slots are etched from the right and left of the proposed patch antenna patch as seen in Fig.5.

From Fig. 5 it is found a shift in the resonance frequency from 4.75 GHz with a conventional rectangular patch. The resonance is shifted to 5.2 GHz with an excellent impedance matching when the truncated patch is used. Therefore, the truncated patch is considered for the proposed antenna design.

3. **Parametric study**

The performance of the proposed antenna is evaluated in terms of $|S_{11}|$ spectra, realized gain, radiation and aperture efficiencies, as well as the far-field radiation patterns before and after introducing the EBG array. A parametric analysis is conducted on the suggested antenna design to determine the optimal antenna performance based on EBG structure. Adjusting the distance between the EBG array structure and the proposed radiating patch antenna is included in this study. Therefore, the EBG array location from the antenna with maximum gain and best aperture efficiency are determined. Moreover, the effects of rotating the EBG array on the antenna performance are discussed in this part also. Changing the separation distances between the EBG unit cells, w1 and w2, from 1 mm to 11 mm, with step of 2 mm, shows significant effects on the $|S_{11}|$ and realized gain spectra as seen in Fig. 6. Changing the dimensions (w1 and w2) change the mutual coupling based capacitance and inductance effects between the EBG unit cells [1]. Therefore, it is found with increase the separation distance between the EBG unit cells the $|S_{11}|$ and realized gain spectra are reduced except the case when the separation distance (w1 and w2) is 1 mm as depicted in Fig. 6.

The effects of changing the position of the EBG array with respect to the antenna (d) are discussed in terms of $|S_{11}|$ and realized gain spectra. Therefore, the distance d is changed from 10 mm to 70 mm with a step of 10 mm. It is found from the obtained results, see Fig. 7, insignificant changes in the

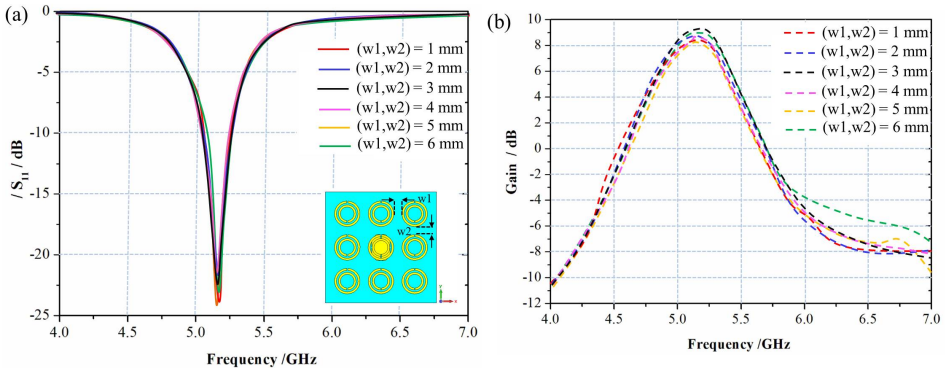

Fig. 6. Parametric study with changing w1 and w2 values: (a) $|S_{11}|$ spectrum and (b) realized gain.

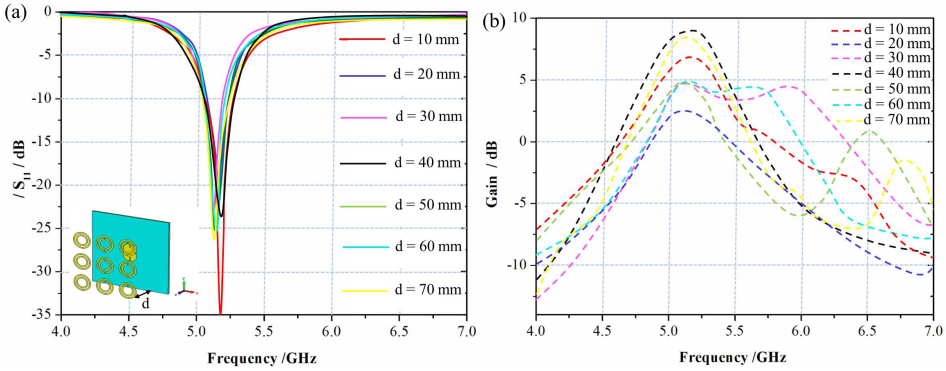

Fig. 7. Changing d:(a) $|S_{11}|$ spectrum and (b) realized gain.

resonant frequency were occurred. However, significant changes are observed in the antenna gain with changing the value of d. It is found a maximum gain can be obtained at d = 40 mm. The maximum obtained gain is found about 8.95 dBi at 5.2 GHz when $|S_{11}|$ = -23 dB.

Varying the EBG array dimensions is studied by changing that from 1×1, 3×3, 5×5, and 7×7. It is observed a significant change in the $|S_{11}|$ spectra and the realized gain, as presented in Fig. 8. It is found with increasing the EBG array up to 3×3, insignificant change in the antenna gain may happen. This is due to the fact of the radiation diffraction limitations from the array edges [25]. While, the deterioration in antenna gain for the case of having a single EBG unit cell could happen due to the high surface impedance on individual EBG [26]. Therefore, it is concluded there is a direct relationship between the antenna gain and the EBG number. For the cases more than one EBG array, the gain improvement is due to the beam focusing [13] . In Table 4, the proposed antenna performance is compared for the proposed cases. It is found that the maximum realized gain can be achieved when the array size is 3×3.

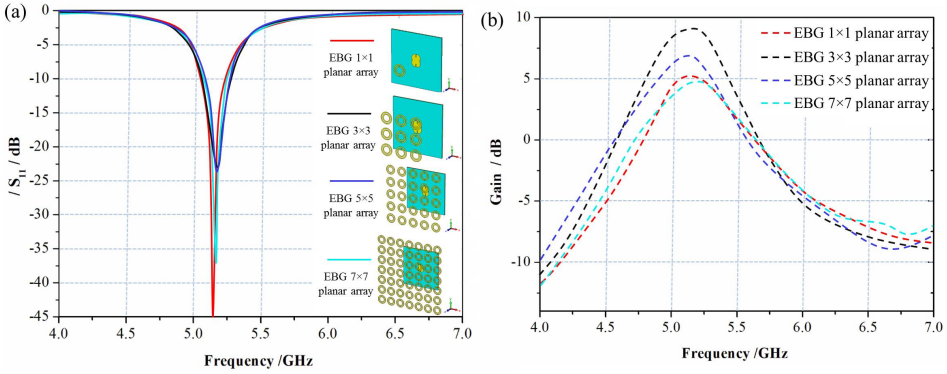

Fig. 8. Effects of the EBG array size in terms of :(a) $|S_{11}|$ spectrum and (b) realized gain.

Table 4

Antenna performance variation with changing the EBG number

EBG Array	Frequency (GHz)	$\|S_{11}\|$(dB)	B.W(MHz)	Gain(dBi)	AE%
1 × 1	5.14	-45	185	5.2	17.8
3 × 3	5.2	-23	213	8.95	43
5 × 5	5.17	-35	177	6.8	14.7
7 × 7	5.16	-36	187	4.78	4.7

Later, the effect of the EBG array rotating on the antenna performance is studied. Fig. 9 shows a notable change in the antenna performance due to the EBG rotation. Therefore, the proposed EBG array is rotated with 0°, 90°, 180°, 270°, and 360°. The $|S_{11}|$ is not affected significantly. However, it is found, that the antenna gain at 90° and 270° is maximally enhanced as can be observed in Fig. 9. This is attributed to the EBG unit cell characteristics change with the angle of orientation [26]. For this, the resonant frequency of the EBG unit cell is tested with the unit cell orientation. It is found a significant shift in the frequency resonance from 5.2 GHz to 7.25 GHz with rotating the EBG unit cell by 90° and 270° as seen in Fig. 9(b).

In order to realize the effect of the substrate material on antenna performance, the authors studied the antenna based on EBG array behavior with different substrate material. The numerical results shows different resonance frequencies with different material as denoted in Fig. 10, it is observed that using different material obtained different resonant frequency with different antenna gain for each substrate. As far as the substrate material availability and its cost is concerned, the authors applied FR-4 material as antenna substrate because of its low cost and its abundance availability in our Printed Circuit Board (PCB) Prototype Manufacturer Lab. Based on this choice an optimal antenna design with EBG array performances can be achieved in terms

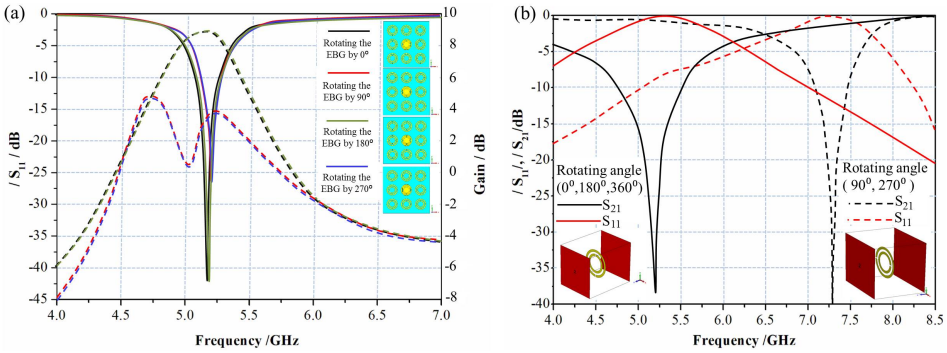

Fig. 9. (a)The effect of rotating the (a) EBG planar array, and (b) EBG unit cell .

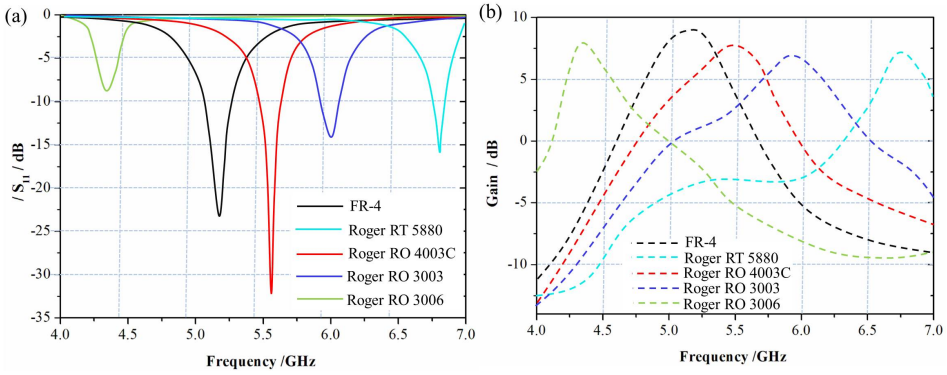

Fig. 10. Effects changing the substrate material on the antenna performance in term of (a) $|S_{11}|$ and (b) antenna gain.

of $|S_{11}|$, antenna radiation and aperture efficiency, and boresight antenna gain, by using FR-4 as substrate materials.

4. **Antenna performance**

In order to characterize the antenna performance, a numerical analysis is performed in terms of $|S_{11}|$ spectrum, radiation and aperture efficiencies, boresight gain before and after introducing the EBG array structure. Figure 11 shows the influences of adding the EBG array to the antenna performance. A significant enhancement in the antenna gain is caused by adding the EBG array. The antenna gain is improved from 3.4 dBi to 8.95 dBi at 5.2 GHz due to focusing beam width from 99° to 26.7°. Besides that, an observable improvements are obtained in terms of bandwidth and radiation efficiency.

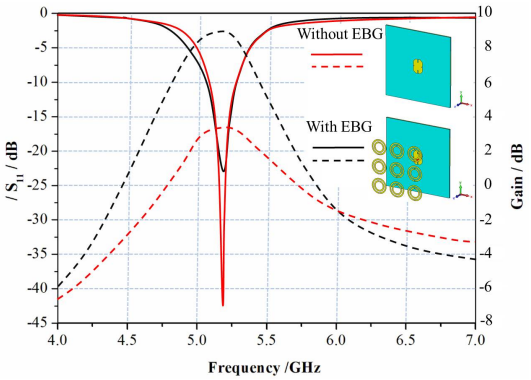

Fig. 11. Antenna performance in terms of $|S_{11}|$ spectra and realized gain before and after the EBG array.

As far as the antenna aperture efficiency is concern, the authors calculated the antenna gain as a function of aperture efficiency with and without EBG structure by using formula 3 [1]:

$$G = \frac{4\pi A\eta}{\lambda^2} \tag{3}$$

G is the proposed antenna gain (unit less ratio), λ is the wave length at 5.2 GHz, η is the antenna aperture efficiency, and A is the proposed antenna physical aperture area. Thus by using equation 3, the aperture efficiency without and with EBG structure of the proposed antenna are represented by equations 4 and 5, respectively:

$$\eta = \frac{10^{\frac{3.4(dBi)}{10}} \times (57.7)^2}{4\pi(70 \times 70)} = 12\% \tag{4}$$

$$\eta = \frac{10^{\frac{8.95(dBi)}{10}} \times (57.7)^2}{4\pi(70 \times 70)} = 43\% \tag{5}$$

Which means, that only 12 % of the power hitting the (70×70) square millimeter area is available at the feed point and the 88 % is lost for the proposed antenna without EBG. While after introduced the EBG that 43 % of the power hitting the (70×70) square millimeter area is available at the feed point and the 53 % is lost. Therefore, η is improved from 12% for the antenna without EBG array to 43% after the EBG array introduction. As shown from equations (4) and (5), the effective aperture only 12 % of the collecting area of the proposed antenna without EBG and after introduced the EBG structure the collecting area of the antenna is improved to 43 %. Table 6 summarizes the proposed antenna performance before and after the introduction of the EBG array.

The simulated 2D radiation patterns are shown in Fig. 12, it is observed that the proposed antenna without the EBG array has a directivity of 12 dBi

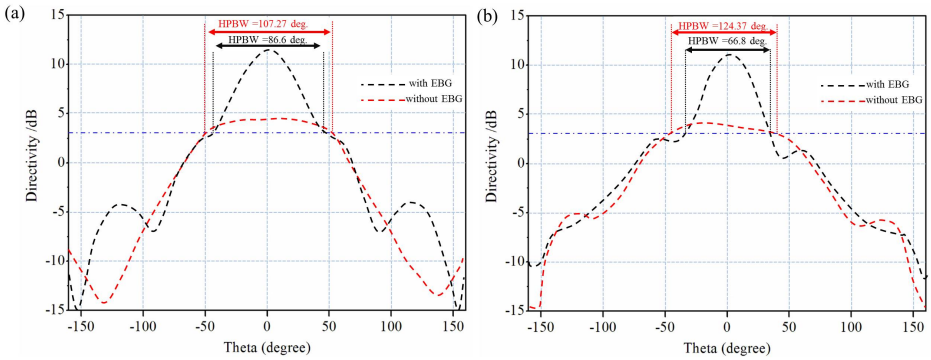

Fig. 12. The proposed antenna's simulated cartesian radiation pattern with and without EBG (a) E-plane, (b) H-plane.

and a HPBW θ_E about 107.27° in the E-plane and HPBW (θ_H) of 124.37° in the H-plane as seen in Fig. 12. However, due to the EBG array introduction, the HPBW is narrowed down to 91.14° at θ_E and to 64.49° at θ_H. These results indicate that the EBG array acts as a perfect lens to focus the electromagnetic waves to paraxial rays [24], as explained in equation 6 from [19].

$$G \simeq \frac{30000}{\theta_E \theta_H} \tag{6}$$

The antenna gain is increased by 5.55 dBi, and the beam width is narrowed by approximately 60% with respect to the proposed antenna before introduce the EBG structure.

The antenna 3D radiation patterns with and without EBG array at 5.2 GHz are compared in Fig. 13. It is observed that the patterns of antenna radiation are sharp and focusing in the boresight direction to accommodate the Wi-Max applications.

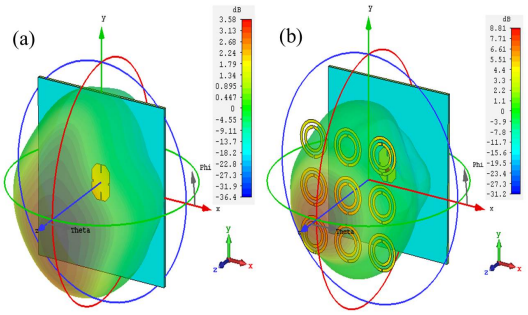

Fig. 13. 3D radiation patterns of the proposed antenna (a) without EBG and (b) with EBG.

5. **Measurements and discussion**

For experimental measurements, the proposed EBG array and microstrip patch antenna are fabricated using PCB technology. RF anechoic chamber is used with a Vector Network Analyzer (VNA) analyzer to characterize the proposed antenna performance. The antenna radiation patterns are measured beyond the far-field distance around 5 m with respect to the transmit antenna inside the anechoic chamber. The fabricated prototype is shown in Fig. 14(a). Four identical plastic stands are used to hold the EBG array.

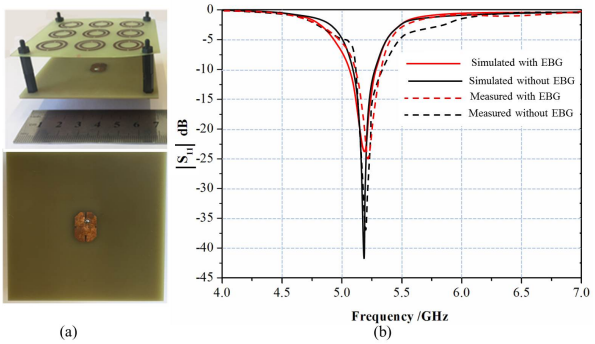

Fig. 14. (a)The fabricated prototype , (b) simulated and measured $|S_{11}|$ with/without EBG

After conducting the measurements, an excellent matching are found between the simulated and measured results in terms of $|S_{11}|$ spectra as depicted in Fig. 14(b).

The simulated and measured 2D antenna radiation patterns at 5.2 GHz in E-plane and H-plane at 5.2 GHz before and after introduce the EBG structures are depicted in Fig. 15. It is noticed from the radiation patterns, the main beam width is improved at 5.2 GHz after introducing the EBG array.

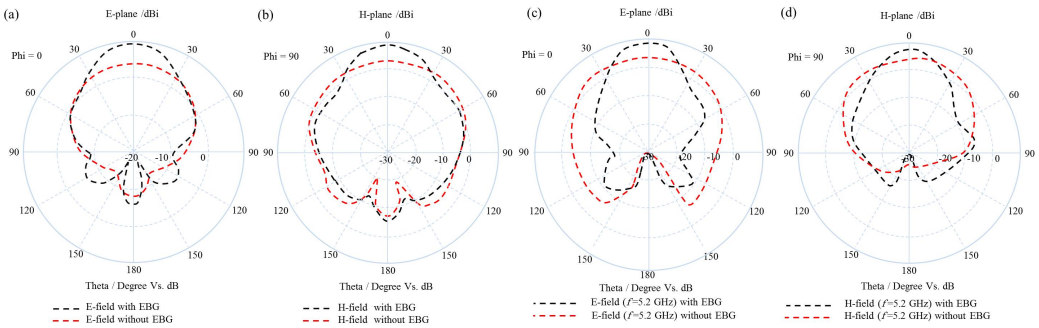

Fig. 15. The simulated (a), (b) and measured (c), (d) 2D far-field radiation patterns in the E-plane and H-plane, before and after introducing the EBG structure.

Table 7

A comparison between the proposed antenna and other published work

Referance	Technique	Array	Layer	Substrate	Size $(mm)^2$	Frequency (GHz)	Gain(dBi)	Complexity
[9]	UCPBG	9×9	1	Taconic	360 ×360	2.6	7.8	High
[10]	CSRR	2×2	1	FR4	40 ×46	2.45	5.93	Moderate
[11]	SRR	4×2	1	FR4 epoxy	100 ×45	3.5-11	7-10	Moderate
[12]	HSRR	1×3	1	FR4	19.4 ×23.8	UWB	1.5-3.88	Low
[13]	SRR	7×7	4	RT5880	49 ×49	5.9	14.23	High
[14]	SRR	2×4	1	FR-4	22 ×26	UWB	3	Moderate
[15]	SRR	1×3	4	FR4	84 ×98	0.947	4.87	High
[16]	EBG	5×5	1	RO3203	240 ×240	2.45	11.1	Moderate
[17]	SRR	3×1	1	Diamond	66.4 ×66.4	multiband	7	High
[18]	TSRR	3×3	3	FR4	N	10.67	11.5	High
[19]	SRR	4×5	6	FR4	122 ×342	3.2	15.42	Moderate
[20]	CSRR	2×1	1	FR4	50 ×50	2.3,2.4	0.62,1.57	High
[21]	SRR	2×1	1	FR4	30 ×31	2.33,3.73,5.55	2.25	Low
This work	EBG	3×3	1	FR4	70 ×70	5.2	8.95	Low

The current study is compared with other literature studies with different models to highlight the proposed antenna design's feasibility. The results obtained from this work are compared in Table 7 with other published works. With a single layer of EBG structure, the proposed BEG-based antenna offers more significant boresight gain improvements than other metamaterials solution in [9], [13], [15], [18], and [19], that are based on more than one layer. Therefore, the proposed antenna configuration is less complicated than other works of literature in the development process. In comparison, the proposed antenna shows a larger increase in antenna gain compared to the conventional antenna design[9]-[21].

Therefore, the proposed antenna design provides high gain, low manufacturing cost, and low profile, making the designed antenna suitable for several wireless applications in particular Wi-MAX applications.

6. Conclusions

In this paper, a single layer of a 3×3 EBG array is invented to cover a truncated patch antenna to improve the antenna performances is investigated. For this, the patch antenna and the EBG layer are printed on FR-4 substrates with a thickness of 1.6 mm and 0.55 mm, respectively. Numerical simulations based on CSTMWS are performed to design the EBG unit cell, EBG array, and the microstrip antenna. Through several parametric studies, the proposed antenna design based on the EBG array is obtained with the optimal performances in terms of $|S_{11}|$, boresight gain, bandwidth, and antenna radiation and aperture efficiencies. An enhancement in the boresight gain from 3.4 dBi to 8.95 dBi is achieved at 5.2 GHz after introduce the EBG structure. This improvement is mainly attributed to the beam focusing and reducing the beam width in boresight direction. The proposed EBG layer

operation is discussed as a perfect lens after conducting several parametric studies to optimize the EBG unit cell, EBG array, and antenna design numerically. The proposed antenna based on EBG structure is fabricated, measured and tested. An excellent agreement has been observed between the simulated and measured results. Finally, the simulated and measured results confirm that the EBG array significantly improves antenna performance. Unlike most of the antenna gain improvement methods that are previously published, the proposed approach used a single layer of metamaterials to increase the gain and enhance the aperture efficiency, HPBW, and the bandwidth of the proposed antenna. The aperture efficiency is increased from 12% to 43%, HPBW is improved from 107.27° to 86.6° in E-plane and for the H-plane from 124.37° to 66.8°. The antenna bandwidth is enhanced from 188 MHz to 244 MHz.

Acknowledgement

The research reported in this paper was supported by the BME NC TKP2020 grant of NKFIH Hungary.

REFERENCES

[1] *C. Caloz, T. Itoh*, Electromagnetic metamaterials: transmission line theory and microwave applications, John Wiley and Sons, 2005.

[2] *V.G Veselago*, Electrodynamics of substances with simultaneously negative and, Usp. Fiz. Nauk **92** (1967) 517.

[3] *E. Yablonovitch*, Inhibited spontaneous emission in solid-state physics and electronics, Physical review letters **58** (20) (1987) 2059.

[4] *S. John*, Strong localization of photons in certain disordered dielectric superlattices, Physical review letters **58** (23) (1987) 2486.

[5] *Y. Alnaiemy, T. A. Elwi, and L. Nagy*, Mutual coupling reduction in patch antenna array based on ebg structure for MIMO applications, Periodica Polytechnica Electrical Engineering and Computer Science **63** (4) (2019) 332–342.

[6] *T. A. Elwi, Y. Alnaiemy*, Miniaturized wide band folded microstrip antennas based metamaterials (2018).

[7] *C. Caloz, T. Itoh*, Novel microwave devices and structures based on the transmission line approach of meta-materials, in: IEEE MTT-S International Microwave Symposium Digest, 2003, **Vol. 1**, IEEE, 2003, pp. 195–198.

[8] *E. K. Hamad, G. Nady*, Bandwidth extension of ultra-wideband microstrip antenna using metamaterial double-side planar periodic geometry, Radioengineering **28** (1) (2019) 25.

[9] *T. A. Elwi, H. M. Al-Rizzo, N. Bouaynaya, M. M. Hammood, Y. Al Naiemy*, Theory of gain enhancement of UC-PBG antenna structures without invoking maxwell's equations: An array signal processing approach, 350 Progress in Electromagnetics Research **34** (2011) 15–30.

[10] *R. Pandeeswari, S. Raghavan*, Microstrip antenna with Complementary SRR loaded ground plane for gain enhancement, Microwave and Optical Technology Letters **57** (2) (2015) 292–296.

[11] *Y. Sun, H. Jin*, Design of broadband endfire antenna with SRR structures, in: 2019 IEEE International Conference on Computational Electromagnetics (ICCEM), IEEE, 2019, pp. 1–3.

[12] *M. T. Islam, F. B. Ashraf, T. Alam, N. Misran, K. B. Mat*, A compact ultrawideband antenna based on hexagonal SRR for ph sensor application, Sensors **18** (9) (2018) 2959.

[13] *D. Gangwar, S. Das, R. L. Yadava*, Gain enhancement of microstrip patch antenna loaded with SRR based relative permeability near zero as superstrate, Wireless Personal Communications **96** (2) (2017) 2389–2399.

[14] *M. Mahmud, M. T. Islam, N. Misran, M. J. Singh, K. Mat, et al*, A negative index metamaterial to enhance the performance of miniaturized UWB antenna for microwave imaging applications, Applied Sciences **7** (11) (2017) 1149.

[15] *C. Ng, K. Devi, C. Chakrabarty, N. M. Din, C. Kwong*, Gain enhancement of microstrip patch antenna using low loss negative refractive index metamaterial superstrate, Journal of Telecommunication, Electronic and Computer Engineering (JTEC) **9** (1-4) (2017) 95–99.

[16] *Y. Alnaiemy, T. A. Elwi, N. Lajos*, microstrip antenna gain using a novel EBG lens based on a single layer, in: 2018 11th International Symposium on Communication Systems, Networks and Digital Signal Processing (CSNDSP), IEEE, 2018, pp. 1–4.

[17] *S. K. Patel, C. Argyropoulos*, Enhanced bandwidth and gain of compact microstrip antennas loaded with multiple corrugated Split Ring Resonators, Journal of ElEctromagnEtic WavEs and applications **30** (7) (2016) 945–961.

[18] *A. K. Panda, A. Sahu*, An investigation of gain enhancement of microstrip antenna by using inhomogeneous triangular metamaterial, in: 2011 International Conference on Computational Intelligence and Communication Networks, IEEE, 2011, pp. 154–157.

[19] *N. N. Yoon, N. Ha-Van, C. Seo*, High-gain and wideband aperture coupled feed patch antenna using four Split Ring Resonators, Microwave and Optical Technology Letters **60** (8) (2018) 1997–2001.

[20] *S. Dey, S. Mondal, P. P. Sarkar*, Single feed circularly polarized antenna loaded with Complementary Split Rring Rresonator (CSRR), Progress In Electromagnetics Research **78** (2019) 175–184.

[21] *M. Hasan, M. Rahman, M. R. I. Faruque, M. T. Islam, M. U. Khandaker, et al*, Electrically compact srr-loaded metamaterial inspired quad band antenna for bluetooth/WiFi/WLAN/WiMAX system, Electronics **8** (7) (2019) 790.

[22] *D. R. Smith, N. Kroll*, Negative refractive index in left-handed materials, Physical review letters **85** (14) (2000) 2933.

[23] C. M. Studio, 3D EM simulation software, Computer Simulation Technology (2017).

[24] *T. A. Elwi, D. A. Jassim, H. H. Mohammed*, Novel miniaturized folded UWB microstrip antenna-based metamaterial for rf energy harvesting, International Journal of Communication Systems **33** (6) (2020).

[25] *H. M. AlSabbagh, T. A. Elwi, Y. Al-Naiemy, H. M. Al-Rizzo*, A compact triple-band metamaterial-inspired antenna for wearable applications, Microwave and Optical Technology Letters **62** (2) (2020) 763–777.

[26] *T. A. Elwi*, A further investigation on the performance of the broadside coupled rectangular split ring resonators, Progress In Electromagnetics Research **34** (2012) 1–8.